THE ROLES OF FRICTION AND DEFORMATION ON IMPACT HEATING K. Kurosawa[1] and H. Genda[2], [1]Planetary Exploration Research Center, Chiba Institute of Technology (2-17-1, Tsudanuma, Narashino, Chiba 275-0016, Japan, E-mail: kosuke.kurosawa@perc.it-chiba.ac.jp), [2]Earth-Life Science Institute, Tokyo Institute of Technology (2-12-1 Ookayama, Meguro-ku, Tokyo 152-8550, Japan).

Summary: We investigated the effects of friction and deformation in shock-generated damaged rocks using the iSALE shock physics code. Conversion from kinetic to internal energy in the target with strength during pressure release due to plastic work becomes significant for low-velocity impacts (10 km s^{-1}). The impact velocity required for the reset of ^{40}Ar–^{36}Ar ages and incipient melting of the target with the 0.1 projectile mass is reduced from 8 to 2 km s^{-1} and 10 to 6 km s^{-1}, respectively, when material strength is considered. This work has been accepted for publication in *Geophysical Research Letters*. [1]

Introduction: Mutual collisions between two bodies at speeds of several km s^{-1} cause significant heating of their surface materials [e.g., 2], resulting in the reset of ^{40}Ar–^{36}Ar age and the generation of impact melts. Since the degree of impact heating depends strongly on the impact velocity, analyses of such heated samples allow us to decode the impact environment in the solar system through its history [e.g., 3]. Understanding the impact velocities required for incipient and complete melting is necessary to extract the information about the impact environment from the occurrence of the Ar loss and melting in geologic samples.

An analytical method, often referred to as the entropy matching method [e.g., 2], has been widely used to obtain the peak pressures required for the incipient and complete melting by assuming that the shocked materials expand adiabatically (dS = 0, where S is specific entropy) to the reference volume. It is widely believed that the isentropic assumption is valid for relatively-high velocity impacts.

Recent laboratory [4] and numerical [5] experiments have demonstrated that the degree of impact heating in the target with strength could be higher than the prediction by the entropy matching method. Such unexpected additional heating has not been recognized in a number of one-dimensional shock-recovery experiments, possibly because the amount of permissible volumetric strain in the 1-D experiments is much smaller than the case of 3-D deformation during natural impacts. Although the previous studies [4, 5] did not address how the material strength enhances impact melting, their new findings are important in terms of the decode of the impact environment.

In this study, we investigated how material strength affects the degree of impact heating using the iSALE shock physics [6-8] code combined with a simple well-established constitutive model.

Numerical model: The strength model for rocks [7, 9] and ANEOS [15] for dunite [16] were applied for both projectile and target. Figure 1a shows the stress-strength curve employed in our numerical model. We used the Lundborg strength model [10] for intact rocks and the Coulomb friction law for damaged rocks. A damage parameter D was introduced to combine the two models depending on temporal volumetric strain. Since the damage parameter D near the impact point reaches unity immediately after the shock-wave arrival, we focused only on the effects of yield strength of the damaged rocks Y_d on the additional heating. The yield strength Y_d is well known as the Coulomb friction law $Y_d = Y_{coh}+\mu_{dam}P$, where Y_{coh}, μ_{dam}, and P are the cohesion, internal friction and temporal pressure, respectively. Although we varied μ_{dam} from 10^{-4} to 0.6 to systematically explore the role of Y_d on impact heating [1], the results in the cases of purely hydrodynamic and μ_{dam} = 0.6 are only presented in this abstract. A thermal softening model was also used to reproduce the strength behavior around the melting temperature. The more details can be found in [1]. Figure 1b shows the Hugoniot curve on an entropy-pressure (S-P) plane. The entropies required for the rapid Ar loss S_{Ar}, incipient and complete melting S_{im} and S_{cm} were determined based on the temperatures for such changes at 10^5 Pa.

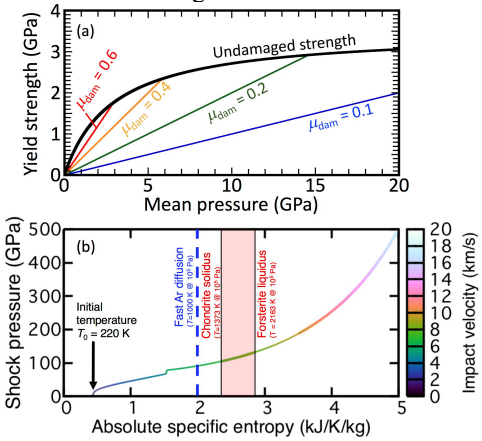

Fig. 1. (a) The stress-strength curve used in the computation. (b) The Hugoniot curve for dunite. The entropies required for Ar loss, incipient and complete melting are indicated as vertical lines.

Calculation conditions: We only considerd vertical impacts of spherical projectiles onto flat targets in cylindrical coordinate. We divided a projectile into 50 cells per projectile radius. The impact velocity v_{imp} was

varied from 1 to 20 km/s. A uniform initial temperature 220 K was assumed. Lagrangian tracers were inserted into computational cells. We stored the temporal spatial position, pressure, and entropy of each tracer.

Data analyses: We calculated the mass experiencing rapid Ar loss, M_{Ar} and the melting mass M_{melt} using the tracers. M_{Ar} was calculated as the sum of the tracer mass m for $S > S_{Ar}$; M_{melt} was calculated using the lever rule. The melts produced by the partial melting of the heated targets were also included in our calculation.

Results: Figures 2ab show snapshots at 6 km s^{-1} without strength and for μ_{dam} = 0.6, respectively. The entropies for μ_{dam} = 0.6 are much higher than those in the hydrodynamic case. Figures 2cd show temporal variations in entropy in the *S*–*P* plane shown in Figs 2a and 2b, respectively. We found that the entropy gradually increases during pressure release in the case of μ_{dam} = 0.6 (Fig. 2d). Some of the tracers eventually exceed S_{Ar} and S_{im}. In contrast, Fig. 2c shows the entropy is mostly preserved during pressure release in the hydrodynamic case.

Figures 3ab show M_{Ar} and M_{melt} as functions of v_{imp}, respectively. We estimated the velocities when M_{Ar} and M_{melt} exceed 10 wt% of the projectile mass as the impact-velocity thresholds v_{Ar} and v_{melt} in this study. The rate of increase in M_{Ar} and M_{melt} decreases with increasing v_{imp} because the thermal softening effectively occurs for relatively high-velocity impacts. The v_{Ar} and v_{melt} are estimated to be 8 and 10 km/s, respectively, in the hydrodynamic case. For μ_{dam} = 0.6, v_{Ar} and v_{melt} significantly decrease to 2 and 6 km/s, respectively.

Discussion and Conclusions: The additional heating in the targets with strength becomes obvious for relatively-low velocity impacts. This comes from the fact that the impact-induced melting occurs during pressure release from the peak shock state to the reference state. Since the shocked materials are in a solid state under relatively-low shock compression, friction and plastic deformation produce the additional heat in an impact-driven flow field. The plastic work $e_{strength}$ is roughly expressed as $e_{strength} = \varepsilon Y_d/\rho$, where ρ and ε are the density and volumetric strain, respectively. The expected temperature rise ΔT is approximated as $\Delta T = e_{strength}/C_p$, where $C_p \sim$ 1000 J/K/kg is the isobaric specific heat. When we assumed $\varepsilon \sim 1$ and time-independent, ΔT is estimated to be $\sim 10^3$ K at a temporal pressure of 10 GPa. Thus, the plastic work during the pressure release is expected to be sufficient to produce the additional heating observed in our numerical experiments.

The velocity thresholds v_{Ar} and v_{melt} for geological materials, as obtained by the entropy matching method, would need to be significantly revised using shock physics codes combined with constitutive models.

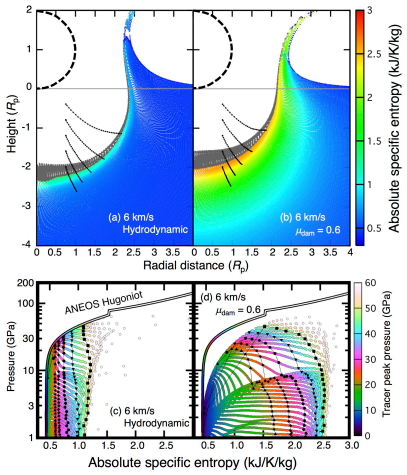

Fig. 2. (Upper) Snap shots. (Lower) Thermodynamic histories of the tracers initially located at a horizontal distance of 0.76 projectile radius. The trajectories and *S*-*P* histories of selected five tracers are also shown as black filled circles.

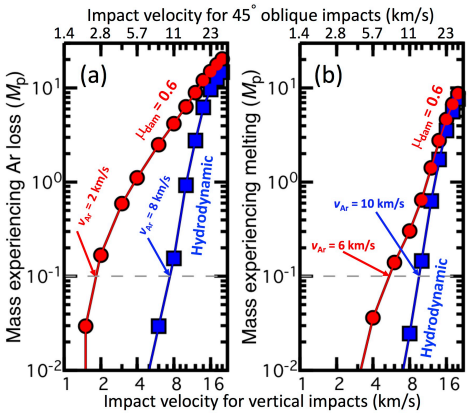

Fig. 3. (a) M_{Ar} and (b) M_{melt} as a function of impact velocity. The impact velocity for oblique impacts are also shown on upper X axis.

In addition, our results imply that we should choice consti tutive models for shock physics codes with close attention to details.

Acknowledgements: We appreciate the developers of iSALE, including G. Collins, K. Wünnemann, B. Ivanov, J. Melosh, and D. Elbeshausen.

References: [1] Kurosawa, K. & Genda H. (2018), *GRL*, In press. [2] Ahrens, T. J. & O'Keefe, J. D. (1972), *The Moon*, **4**, 214-249. [3] Marchi S. et al. (2013), *Nature Geoscience*, **6**, 303-307. [4] Kenkmann T. et al. (2013), *MaPS*, **48**, 150-164. [5] Quintana, S. N. et al. (2015), *Proc. Eng.*, **103**, 499-506. [6] Amsden A. A., et al. (1980) *LANL Report* LA-8095. 101 p. [7] Ivanov B. A., et al. (1997), *IJIE*, 20, 411. [8] Wünnemann, K., et al. (2006), *Icarus*, 180, 514. [9] Collins G. S. et al. (2004), MaPS, 39, 217-231. [10] Lundborg, N. (1968), *Int. J. Rock Mech. Min. Sci.*, **5**, 427-454.